INTERNATIONAL JOURNAL OF ADAPTIVE CONTROL AND SIGNAL PROCESSING, VOL. 11, 49–63 (1997)

NEW MODELS FOR BACKLASH AND GEAR PLAY

MATTIAS NORDIN
Optimization and Systems Theory, The Royal Institute of Technology, S-100 44 Stockholm, Sweden

JOHANN GALIC'
Metals Division Department HUA, ABB Industrial Systems AB, S-721 67 Västerås, Sweden

AND

PER-OLOF GUTMAN
Faculty of Agricultural Engineering, Technion, Haifa 32000, Israel

SUMMARY

Backlash is the most important non-linearity that limits the performance of speed control in industrial drives and is an important impediment to position control as well. A new simple model based on phase plane analysis is derived for an elastic shaft with internal damping connected to a backlash The model is extended to include the case of a so-called flexible coupling, where some of the backlash gap is filled with rubber. Extensive measurements on an industrial drive with a flexible coupling are compared with simulations and fit very well. With internal damping the classical dead-zone model gives an unphysical behaviour of the dynamics. However, the new model converges to the classical dead-zone model when the damping tends to zero.

KEY WORDS backlash; drive trains; gear play; non-linear control

1. INTRODUCTION

In industrial drives, elements such as gearboxes and flexible couplings introduce backlash. For instance, a commonly used flexible coupling gives a backlash of about 10°. This gap is then partly filled with rubber.

Traditionally, backlash connected with an elastic shaft has been modelled as a dead-zone (see e.g. References 1–4, 20–22), which gives the output shaft torque as a function of the displacement between the input and output shafts, $\theta_d = \theta_1 - \theta_2$. Here the classical dead-zone model is shown to be wrong when the shaft has non-negligible internal damping: the transmitted torque is erroneously computed, even with the wrong sign. It is not possible to model the shaft damping as an equivalent motor damping and/or load damping or with the damping included in series with the dead-zone.[5–9]

Another traditional backlash model is the hysteresis model,[10,11] where the output position of the backlash is given as a function of the time history of the input position. When the output position is influenced by disturbances, however, the causality is lost. In our model, as well as in the dead-zone model, all disturbances enter at the input of the model.

CCC 0890–6327/97/010049–15

This paper first presents a new exact backlash model that takes the internal damping into account. After simplification the torque is found to be a function of the displacement θ_d and its time derivative. The model is extended to the case of a flexible coupling, i.e. when part of the backlash gap is filled with rubber.

It should be pointed out that the shaft moment of inertia is assumed to be negligible in comparison with the motor and load moments of inertia. This is a valid assumption in most industrial speed control systems and in many robotics and servo control applications.

The paper, which is a shortened version of Reference 12, is organized as follows. In Section 2 the physical behaviour of an inertia-free shaft is analysed. After simplification the *phase plane model* is derived. Analysis and simulations are then used to compare the physical system, the phase plane model and the dead-zone model. In Section 3 we extend the phase plane model to the case of a flexible coupling with rubber.

In Section 4 extensive measurements and simulations of a two-mass system connected with a flexible coupling are shown to be strikingly similar.

2. BACKLASH MODELS

In this section the behaviour of an inertia-free elastic shaft with backlash is analysed. Based on phase plane analysis, an approximate shaft model is derived. Comparisons between the new model, the exact solution and the classical dead-zone model are presented, with both analysis and simulations.

2.1. *Physical model for the shaft torque T*

Consider an inertia-free shaft consisting of a backlash gap 2α (rad) and a spring with elasticity k (Nm rad^{-1}) and viscous damping c (Nm rad^{-1} s^{-1}) as in Figure 1. Note that with an inertia-free shaft the torque T on the left side is equal to the torque T on the right side in the figure. Denote time (sec) by t; when convenient, the explicit time dependence is supressed. Let $\theta_1(t)$ (rad) be the angle of the motor, $\theta_3(t)$ (rad) the angle of the driving axis at the backlash and $\theta_2(t)$ (rad) the angle of the driven member. The goal is to acquire the torque T (N m) as a function of the *displacement* defined as $\theta_d(t) = \theta_1(t) - \theta_2(t)$ and its time derivative $\dot{\theta}_d(t) = \dot{\theta}_1(t) - \dot{\theta}_2(t)$, i.e. without using the state $\theta_3(t)$. Define the *shaft twist* $\theta_s(t) = \theta_1(t) - \theta_3(t)$ and the *backlash angle* $\theta_b(t) = \theta_3(t) - \theta_2(t)$, defined symmetrically within the backlash gap such that $|\theta_b| \leq \alpha$. An examination of the model in Figure 1 gives an exact expression for T using $\theta_s = \theta_d - \theta_b$:

$$T(t) = k\theta_s + c\dot{\theta}_s = k(\theta_d - \theta_b) + c(\dot{\theta}_d - \dot{\theta}_b) \tag{1}$$

The impact when the backlash gap is closed is assumed to be inelastic. There can be contact between the driving and the driven member on either side of the backlash. Define the case with $\theta_b = \alpha$ and $\dot{\theta}_b = 0$ as *right contact* and the case with $\theta_b = -\alpha$ and $\dot{\theta}_b = 0$ as *left contact*. We say that there is *contact* if there is either *right contact* or *left contact*.

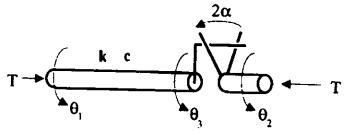

Figure 1. The physical system: a shaft connected to a backlash

It holds that $T>0$ implies *right contact*, because otherwise no positive torque could be transmitted. Together with (1) this gives

$$T>0 \quad \Rightarrow \quad T=k(\theta_d-\alpha)+c\dot{\theta}_d>0 \tag{2}$$

Similarly $T<0$ implies *left contact*. Together with (1) this gives

$$T<0 \quad \Rightarrow \quad T=k(\theta_d+\alpha)+c\dot{\theta}_d<0 \tag{3}$$

Logical negation of (2) and (3) yields

$$\begin{cases} k\theta_d+c\dot{\theta}_d \geqslant -k\alpha \quad \Rightarrow \quad T \geqslant 0 \\ k\theta_d+c\dot{\theta}_d \leqslant k\alpha \quad \Rightarrow \quad T \leqslant 0 \end{cases} \tag{4}$$

respectively. Equations (1)–(4) give

$$\begin{cases} T=0 \quad \text{or} \quad T=k(\theta_d-\alpha)+c\dot{\theta}_d, \quad \theta_d+(c/k)\dot{\theta}_d>\alpha \\ \qquad\qquad T=0, \quad |\theta_d+(c/k)\dot{\theta}_d| \leqslant \alpha \\ T=0 \quad \text{or} \quad T=k(\theta_d+\alpha)+c\dot{\theta}_d, \quad \theta_d+(c/k)\dot{\theta}_d<-\alpha \end{cases} \tag{5}$$

which can be expressed in terms of the phase plane $(\theta_d, \dot{\theta}_d)$; see Figure 2(a). In the non-shaded areas of Figure 2(a) the $T=0$ cases of (5) are valid only if there is no contact, because otherwise $\theta_b=\pm\alpha$ and $\dot{\theta}_d=0$, which would cause $T\neq 0$; see (1)–(3). This means that if it were known whether or not there is contact, T could be computed exactly from θ_d and $\dot{\theta}_d$. This problem can then be solved by first analysing when contact is lost and then when contact is achieved.

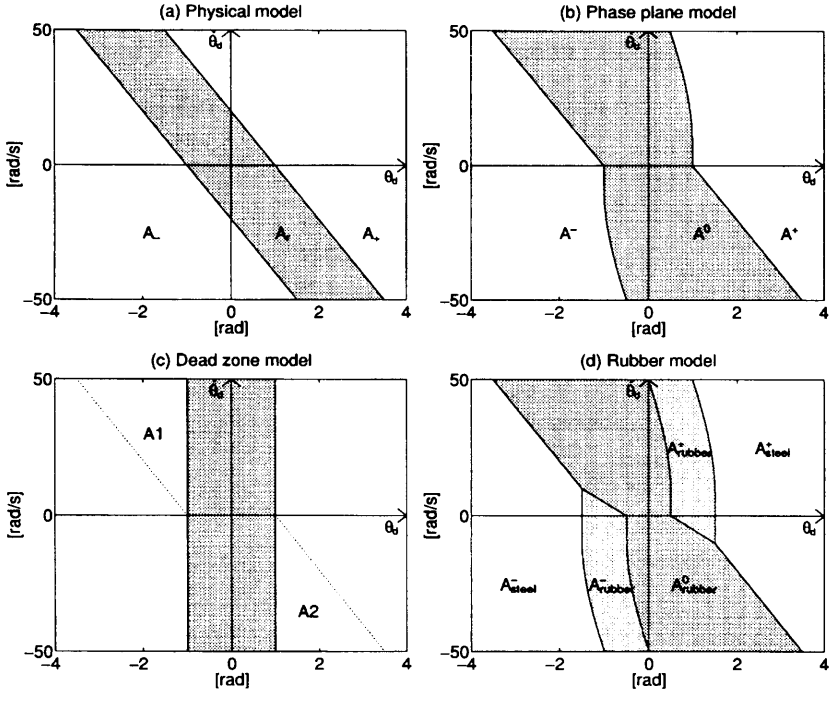

Figure 2. Phase plane plots of T for $\alpha=1$ rad, $k/c=0{\cdot}1\ \text{s}^{-1}$ and $\beta=0{\cdot}5$ rad: (a) the exact model (5); (b) the phase plane model (23); (c) the dead-zone model (26); (d) the rubber model (40)

Define the following areas of the phase plane in Figure 2(a):

$$A_+ = \{(\theta_d, \dot{\theta}_d): k\theta_d + c\dot{\theta}_d \geq k\alpha\} \tag{6}$$

$$A_r = \{(\theta_d, \dot{\theta}_d): |k\theta_d + c\dot{\theta}_d| < k\alpha\} \tag{7}$$

$$A_- = \{(\theta_d, \dot{\theta}_d): k\theta_d + c\dot{\theta}_d \leq -k\alpha\} \tag{8}$$

where A_r is the interior of the shaded area in Figure 2(a).

Lemma 1

There can be persistent (during a non-zero interval) *right contact* only in A_+ and persistent *left contact* only in A_-.

Proof by contradiction. Assume *right contact* outside A_+. From (1) and (6) it follows that

$$T = \underbrace{k\theta_d + c\dot{\theta}_d}_{< k\alpha} - k\alpha < 0 \tag{9}$$

Hence a persistent negative torque with right contact implies a pull force which is physically impossible. Likewise the case of *left contact* outside A_- is impossible. □

Lemma 2

If the system state $(\theta_d, \dot{\theta}_d)$ at the initial time $t = t_0$ lies in A_+ with $\theta_b(t_0) = \alpha$ (right contact), then $\theta_b(t_1) = \alpha$ for all times $t_1 > t_0$ such that $(\theta_d(t), \dot{\theta}_d(t)) \in A_+$ for all $t \in [t_0, t_1]$. If $(\theta_d(t_0), \dot{\theta}_d(t_0)) \in A_-$ with $\theta_b(t_0) = -\alpha$ (left contact), then $\theta_b(t_1) = -\alpha$ for all times $t_1 > t_0$ such that $(\theta_d(t), \dot{\theta}_d(t)) \in [t_0, t_1]$.

Proof. Right contact in the interior of A_+ together with (1) implies $T > 0$; see (2). As long as there is a positive torque, *right contact* cannot be lost for obvious reasons. On the border of A_+, i.e. with $k\theta_d + c\dot{\theta}_d = k\alpha$, it holds from (5) that $T = 0$ and together with equation (1) this yields

$$\dot{\theta}_b(t) = k(\alpha - \theta_b(t))/c \tag{10}$$

The solution of (10) is

$$\theta_b(t) = \alpha + (\theta_b(t_0) - \alpha)e^{-k(t-t_0)/c} \tag{11}$$

Starting with *right contact*, i.e. $\theta_b = \alpha$, equation (11) becomes a constant $\theta_b = \alpha$, i.e. *right contact* is preserved. A symmetric proof applies for *left contact* and the trajectory in A_-. □

The following theorem can now be proved.

Theorem 1 (release condition)

Assume that $\theta_b(t_0) = \alpha$ or $\theta_b(t_0) = -\alpha$ (contact at time t_0). Contact is lost at the first time $t_1 > t_0$ such that the trajectory $(\theta_d(t), \dot{\theta}_d(t))$ reaches the release set A_r.

Proof. This follows from the fact that right, resp. left, contact cannot be lost in A_+, resp. A_-, and that in A_r, which lies in between, contact is not possible. □

When contact is lost, we know that $T = 0$. Equation (1) then gives

$$\dot{\theta}_d - \dot{\theta}_b = -k(\theta_d - \theta_b)/c \tag{12}$$

whose solution is

$$\theta_b - \theta_d(t) = (\theta_b(t) - \theta_d(t_0))e^{-k(t-t_0)/c} \tag{13}$$

Since θ_d is given, equation (13) gives θ_b. Furthermore, it holds that *contact* is achieved again when $|\theta_b| = \alpha$. An exact solution of the trajectory of θ_b is now given by solving for θ_b as a one-state model. Using equation (12), $|\theta_b| \leq \alpha$ and the release condition, we get

$$\dot{\theta}_b = \begin{cases} \max(0, \dot{\theta}_d + (k/c)(\theta_d - \theta_b), & \theta_b = -\alpha \quad (T \leq 0) \\ \dot{\theta}_d + (k/c)(\theta_d - \theta_b), & |\theta_b| < \alpha \quad \text{(equation (12))} \\ \min(0, \dot{\theta}_d + (k/c)(\theta_d - \theta_b)), & \theta_b = \alpha \quad (T \geq 0) \end{cases} \tag{14}$$

This state equation can be interpreted is a limited integrator with the time derivative $\dot{\theta}_d + (k/c)(\theta_d - \theta_b)$ and limit α. With θ_b and $\dot{\theta}_b$ known from (14) and $\theta_d(t)$ and $\dot{\theta}_d(t)$ given, the torque T is found by (1). We now have a non-linear dynamical system, not a function, that gives the torque T with given θ_d and $\dot{\theta}_d$.

2.2. *Phase plane backlash model*

After an approximation the previous phase plane analysis can be used to get a new model. This model, called the *phase plane model*, will be a function of θ_d and $\dot{\theta}_d$.

Define t_i^r as the ith time the transmitted torque becomes zero, i.e. $T(t_i^r) = 0$ and $T(t_i^r - \varepsilon) \neq 0$, with ε an infinitesimal time. Define also t_i^c as the ith time the transmitted torque becomes non-zero, i.e. $T(t_i^c) = 0$ and $T(t_i^r + \varepsilon) \neq 0$. Let them be defined so that $t_i^r < t_i^c$ and assume without loss of generality that $t_i^r = 0$.

Contact is achieved again when $\theta_b(t_i^c) = \theta_d(t_i^c) - \theta_s(t_i^c) = \pm\alpha$. Equation (13) gives $\theta_b(t_i^c) - \theta_d(t_i^c) = (\theta_d(0) - \theta_b(0))e^{-kt_i^c/c}$. *If* kt_i^c/c is sufficiently large and $|\theta_d(0) - \theta_b(0) - \theta_b(0)| = |\theta_s(0)|$ is sufficiently small, then $\theta_b(t_i^c) - \theta_d(t_i^c) = -\theta_s(t_i^c) \approx 0$, which implies that the shaft has reached steady state. Then contact is achieved for $\theta_d(t_i^c) = \theta_b(t_i^c) = \pm\alpha$.

For large values of $|\theta_s(0)|$ the shaft is not in steady state at t_i^c, so $\theta_s(t_i^c)$ needs to be calculated. Integration gives

$$\dot{\theta}_d(t) = \dot{\theta}_d(0) + \int_0^t \ddot{\theta}_d(s)\,ds, \quad \forall t \in [0, t_i^c] \tag{15}$$

Since $T = 0$ holds here, $\ddot{\theta}_d(t)$ is typically an acceleration produced by the motor and load torques and cannot be *a priori* known. Assume therefore that $\ddot{\theta}_d(t) = 0$, $\forall t \in [0, t_i^c]$, which gives

$$\theta_d(t) = \theta_d(0) + \dot{\theta}_d(0)t, \quad \forall t \in [0, t_i^c] \tag{16}$$

For large values of $|\dot{\theta}_d(0)|$ the integrand of (15) is small relative to the constant term, since the integrand can be assumed bounded and t_i^c will be small.

Consider now the upper half-plane of the phase plane $(\theta_d, \dot{\theta}_d)$, starting at $t_i^r = 0$ on the border of A_r. From Theorem 1 and the definition of A_r it follows that $\dot{\theta}_d(0) = -\alpha)/c > 0$. All motion is now in the positive θ_d-direction; see (15) and (16). Contact will be achieved again when

$$\theta_b(t_i^c) = \alpha = \theta_d(t_i^c) - \theta_s(0)e^{-kt_i^c/c} \tag{17}$$

From (16) it follows that

$$t_i^c = (\theta_d(t_i^c) + \alpha)/\dot{\theta}_d(0) + c/k \tag{18}$$

Now (17) and (18) give

$$f(\theta_d(t_i^c) + \alpha, \dot{\theta}_d(0)) \triangleq (\theta_d + \alpha) + (c\dot{\theta}_d/k)e^{-k(\theta_d+\alpha)/c\dot{\theta}_d - 1} = 2\alpha \tag{19}$$

which corresponds to $\theta_b(t_i^c) - \theta_b(0) = 2\alpha$. For a given value of $\dot{\theta}_d(0)$ there exists a unique solution $\theta^*(\dot{\theta}_d(0)) \in [\alpha - c\dot{\theta}_d(0)/k, \alpha]$ (which is outside A_r) that satisfies $f(\theta^*(\dot{\theta}_d(0)) + a, \dot{\theta}_d(0)) = 2\alpha$.

The backlash will not be in contact, with $T = 0$, as long as $\theta_d < \theta^*(\dot{\theta}_d)$, but when $\theta_d = \theta^*(\dot{\theta}_d)$ is reached, the backlash gap is closed and right contact with $\theta_b(t_i^c) = \alpha$ is achieved. Note that for small values of $c\dot{\theta}_d(0))/k$ the exponential part of (19) will be small and $\theta^* \approx \alpha$. This means that even though the assumption that the integral part of (15) is not neglible holds, the approximation that contact is achieved again for $\theta_d = \theta^*(\dot{\theta}_d)$ is still valid.

Right contact will then be preserved and the linear model $T = k(\theta_d - \alpha) + c\dot{\theta}_d$ given by (5) will hold. T will remain positive until the release condition of Theorem 1 is fulfilled. Note that this can only happen for $\dot{\theta}_d < 0$, i.e. in the lower half-plane, because of the directional constraints in the phase plane $(\theta_d, \dot{\theta}_d)$. By noting that $\theta_d < \theta^*$ is equivalent to $f(\theta_d + \alpha, \dot{\theta}_d) < 2\alpha$ for $k(\theta_d - \alpha) + c\dot{\theta}_d \geq 0$, it holds that there is right contact for $(\theta_d, \dot{\theta}_d) \in A^+$ defined by

$$A^+ = \left\{(\theta_d, \dot{\theta}_d): \begin{cases} f(\theta_d + \alpha, \dot{\theta}_d) \geq 2\alpha, & \dot{\theta}_d > 0 \\ k(\theta_d - \alpha) + c\dot{\theta}_d \geq 0, & \forall \dot{\theta}_d \end{cases}\right\} \tag{20}$$

see Figure 2(b). Symmetry conditions holds for left contact with

$$A^- = \left\{(\theta_d, \dot{\theta}_d): \begin{cases} f(\theta_d - \alpha, \dot{\theta}_d) \leq -2\alpha & \dot{\theta}_d < 0 \\ k(\theta_d + \alpha) + c\dot{\theta}_d \leq 0, & \forall \dot{\theta}_d \end{cases}\right\} \tag{21}$$

Finally we can conclude that there is no contact in A^0 defined by

$$A_0 = \{(\theta_d, \dot{\theta}_d)\} \setminus (A^+ \cup A^-) \tag{22}$$

Remember that the difficult problem was to know whether there was contact or not, which we now have solved approximately. The torque can now be given as a function of θ_d and $\dot{\theta}_d$. The phase plane model is summarized in Figure 2(b) and in equation (23).

$$T_{\text{phase}} = \begin{cases} k(\theta_d - \alpha) + c\dot{\theta}_d, & (\theta_d, \dot{\theta}_d) \in A^+ \\ 0, & (\theta_d, \dot{\theta}_d) \in A^0 \\ k(\theta_d + \alpha) + c\dot{\theta}_d, & (\theta_d, \dot{\theta}_d) \in A^- \end{cases} \tag{23}$$

Note that in (23) T_{phase} is independent of θ_b. Note also that T_{phase} is discontinuous in θ_d for $\theta_d = \theta^*$, which describes what happens when the backlash achieves contact with a non-zero speed difference.

Remark 1

Note that we have made two approximations for the shaft:

(i) The shaft is inertia-free, (Section 2.1) and
(ii) The approximation of $\theta_d(t_i^c)$ given by (20) and (21).

Note, however, that when the shaft is not in backlash contact ($T = 0$) and is only connected to the driving member on one side, approximation (i) might not be valid and (1) and (13) should be at least of second order.

In the derivation of the release condition we used approximation (i) only to prove that contact could not be achieved in A_r and that contact was lost as soon as we reached A_r. It seems that this is still a good approximation, i.e. that contact ceases when $(\theta_d, \dot{\theta}_d)$ leaves the area in the phase plane that gives a non-zero torque. For the exact solution (14) it is critical that (1) or (i) holds also when there is no backlash contact, because this is used to predict when contact is achieved again, and (ii) is not necessarily a worse approximation.

These observations imply that the solutions (14) and (23) are both somewhat inexact with respect to real shafts with inertia.

2.3. The dead-zone model

An often-proposed model, found in almost any basic control course, for analysis and simulations of an elastic shaft with backlash is the classical dead-zone model (see e.g. References 1–4, 10 and 20–22), where the torque is given by

$$T = kD_\alpha(\theta_d) \tag{24}$$

with

$$D_\alpha(x) = \begin{cases} x - \alpha, & x > \alpha \\ 0, & |x| < \alpha \\ x + \alpha, & \theta_d < -\alpha \end{cases} \tag{25}$$

The model of the shaft is here a pure spring, i.e. it is inertia-free and has no internal damping. The shaft is assumed to be in steady state when it is free, i.e. when there is no backlash contact. If internal damping is introduced in the shaft, a commonly used modification of the dead-zone model (see e.g. References 5–9) is that presented in Figure 2(c) and in equation (26). This model will hereinafter be referred to as the *dead-zone model.*

$$T_{\text{dead-zone}} = \begin{cases} k(\theta_d - \alpha) + c\dot{\theta}_d, & \theta_d > \alpha \\ k(\theta_d + \alpha) + c\dot{\theta}_d, & \theta_d < -\alpha \\ 0, & |\theta_d| < \alpha \end{cases} \tag{26}$$

This model, just like the phase plane model, gives the torque $T_{\text{dead-zone}}$ as a function of θ_d and $\dot{\theta}_d$. Compare the phase plane analysis of the physical model (5) with the phase plane analysis of the phase plane model (23) and the dead-zone model (26); see Figure 2. It is seen that $T_{\text{dead-zone}} \neq 0$ in areas A1 and A2 of Figure 2(c), but this violates (5) and Lemma 1! Furthermore, this is a very unphysical model, because $T_{\text{dead-zone}}$ has the wrong sign in areas A1 and A2, where we know from analysis of the physical model that $T = 0$, i.e. the dead-zone model gives a pull force at the side of the backlash where only a push force is possible; see Figure 2(c). A modification of the dead-zone model that does not violate Lemma 1 is given by

$$T = kD_\alpha(\theta_d + c\dot{\theta}_d/k) \tag{27}$$

An interpretation of (27) is that there is always right contact for $(\theta_d, \dot{\theta}_d) \neq A_+$ with $T = k(\theta_d - \alpha) + c\dot{\theta}_d$ and always left contact for $(\theta_d, \dot{\theta}_d) \neq A_-$ with $T = k(\theta_d) + \alpha) + c\dot{\theta}_d$. Compare equations (6)–(8) and (23) and Figures 2(a) and 2(b).

Remark 2

Note that if $k/c \to \infty$, the solution of (13) immediately goes to $\theta_d = \theta_b$, so now approximation (ii) in Remark 1 made for the phase plane model is exact, namely $\theta_s(t_i^c) = 0$. Furthermore, the slope of the left, resp. right, border of A1, resp. A2, goes to $-\infty$ and hence the areas A1 and A2 go to zero, so the phase plane model converges to the classical dead-zone model (24), to which the dead-zone models (26) and (27) also converge.

Hence the phase plane model and the dead-zone models coincide and are an exact description of the torque behaviour when the shaft is modelled as a pure spring without damping.

2.4. *Model simulation comparisons*

Let us compare simulations of the true model (1), (14) the phase plane model (23), the dead-zone model (26) and the revised dead-zone model (27).

In Figure 3 a simulation of the two-mass system with an elastic shaft with internal damping and backlash can be seen. Remember from previous analysis that the release condition is exact for the phase plane model (23) and the revised dead-zone model (27) but bad for the dead-zone model (26), which can clearly be seen in Figure 3: the shaft torque predicted by the dead-zone model is sometimes negative,although only one side of the backlash is touched. Note that the phase plane model torque T_{phase} and the exact torque T almost overlap in the figure.

The ratio $k/c = 100$ gives a half-time of the exponential term in (13) of about $\ln 2/(k/c) \approx 0{\cdot}0069$ s. For this simulation the shortest time between contacts is about 0·05 s and the exponential term will then be diminished by a factor $e^{-0{\cdot}05k/c} = e^{-5} \approx 0{\cdot}0067$. This means that the prediction of when contact is achieved is very good for both (23) and (26) but bad for (27); see Figure 3. Simulations of this kind made the need obvious for a better model than the dead-zone model.

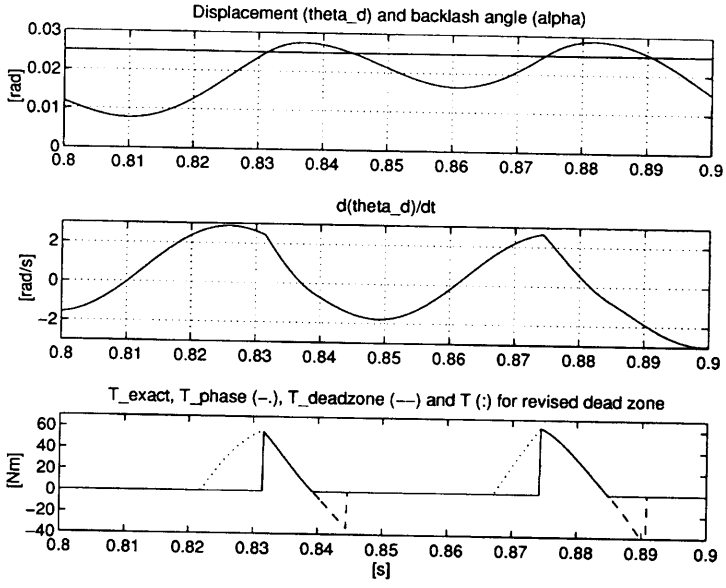

Figure 3. Simulation comparisons

Table I

Backlash model	Integrated torque (10^{-3} N m s)	Error (%)
T from (5)	1·5327	—
T_{phase} from (23)	1·5331	+0·29
T from (26)	0·9486	−38
T from (27)	2·997	+95

The simulation shown in Figure 3 used the mathematical model

$$J_m\ddot{\theta}_m = T_m - T(\theta_d, \dot{\theta}_d) - T_{preload} + a_{dist}\sin(40\pi t)$$
$$J_l\ddot{\theta}_l = T_l + T(\theta_d, \ddot{\theta}_d) + T_{preload}$$
$$\theta_d = \theta_m - \theta_l$$

The exact torque $T(\theta_d, \dot{\theta}_d)$ of (26) and T of (27), are calculated from the θ_d and $\dot{\theta}_d$ given by this simulation. The following parameter values, most of them approximations of a laboratory system at ABB Industrial Systems AB, were used:

$J_m = 0{\cdot}4$ kg m s^{-2}	motor inertia
$J_l = 5{\cdot}6$ kg m s^{-2}	load inertia
$k = 5895$ N m rad^{-1}	shaft elasticity
$c = k \times 0{\cdot}01$ s^{-1} = 58·95 Nm rad^{-1} s^{-1}	inner damping of shaft
$\alpha = 0{\cdot}0025$ rad	backlash angle
$a_{dist} = 19$ N m	disturbance amplitude
$T_{preload} = 19$ N m	preload torque.

One method of comparing the various models is to measure the the integral of the transmitted torque over one cycle, and compare it with the exact model. For the simulation presented in Figure 3, the results given in Table I were obtained;

We can see that the phase plane model fits well to the exact model and that the errors of both dead-zone models are large. This means that even though the revised dead-zone model (27) is exact with respect to the release condition, it predicts badly when contact is achieved and is really no better than the dead-zone model (26).

3. MODEL FOR BACKLASH WITH RUBBER

In an industrial standard flexible coupling there is rubber, in principle as in Figure 4. In this work the specific coupling is manufactured by Benzlers,* but similar couplings are very common in many applications throughout the world. Therefore a model for backlash with rubber is needed. In this section we derive a simple model for an inertia-free elastic shaft with internal damping, connected to a backlash partly filled with rubber. We are not aiming for an exact and complicated model, but rather a workable approximation. The new model is derived as an extension of the phase plane model (23). In Section 4 we simulate a

* Flexible Coupling No. 2245 5268-7 with Rubber Element No. 2245 5195-4, Benzlers AB, Box 922, S-251 09 Helsingborg, Sweden.

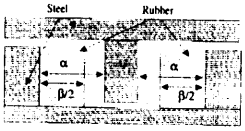

Figure 4. Backlash with rubber

laboratory set-up with the new model and compare it with measurements. Striking similarities are found.

3.1. Shaft model for backlash with rubber

Extensive measurements were performed on a laboratory set-up (described in Section 4). After considering the differences between these measurements and those expected from a set-up with a rubber-free coupling, we were led to introduce the following features into the new model for backlash with rubber.

1. The motor speed measurements seemed to be differentiable for the experiments. Since the motor speed is proportional to the integral of the difference of motor and shaft torques, (42), the shaft torque $T_{\text{rubber}}(\theta_d, \dot{\theta}_d)$ should be modelled as a continuous, not necessarily differentiable, function.
2. The width of the rubber, β(rad), should enter the model.
3. The rubber is soft when not compressed but gets harder as it is compressed. For large twists of the shaft the model should behave as if it were just a steel shaft. This means that $dT_{\text{rubber}}(\theta_s, \dot{\theta}_s)/d\theta_s = k$ and $dT_{\text{rubber}}(\theta_s, \dot{\theta}_s)/d\theta_s = c$ when the rubber is compressed, i.e for large $|\theta_s|$ or equivalently for large $|\theta_d|$.

To achieve features 1–3 above, we extend the phase plane model (23) to include areas of 'rubber effect' in the phase plane $(\theta_d, \dot{\theta}_d)$ as follows.

First assume that right contact is achieved for $\theta_d = \theta^*(\dot{\theta}_d) - \beta/2$, i.e. as predicted by the phase plane model (23), modified by the rubber thickness, see Figure 4 and equation (19) Then introduce a band of thickness β (double the rubber thickness) for $\theta^*(\dot{\theta}_d) - \beta/2 < \theta_d < \theta^*(\dot{\theta}_d) + \beta/2$. In this band let the damping and elasticity k and c vary linearly with θ_d from zero to the parameter values of the steel shaft, which reflects feature 3, i.e. that the rubber gets harder as it is compressed. The choice to let the band of compression be double the rubber thickness is *ad hoc* but, as will be seen later, fits well with measurements.

When right contact is lost for high speed, i.e. for $|\dot{\theta}_d| > c\beta/2k$, assume that there is no time for the rubber to decompress, i.e. no rubber effect. For $|\dot{\theta}_d| < c\beta/2k$ let the damping and elasticity vary linearly from zero to the parameter values of the steel shaft for $\theta_d \in (\alpha - \beta/2 - 2c\dot{\theta}_d/k, \alpha + \beta/2)$; see Figure 2(d). The idea is that when contact is lost for low speeds, there is time for the rubber to decompress somewhat, while for very low speeds it decompresses totally. Let us now formalize these assumptions of rubber behaviour into equations.

Note first that $|\theta_d - \theta^*(\dot{\theta}_d)| < \beta/2 \Leftrightarrow f(\theta_d + \alpha - \beta/2, \dot{\theta}_d) < 2\alpha < f(\theta_d + \alpha - \beta/2, \dot{\theta}_d)$; see the derivation of equation (19). Define now the area of right contact with rubber effect as

$$A^+_{\text{rubber}} = \left\{(\theta_d, \dot{\theta}_d): \begin{bmatrix} f(\theta_d + \alpha - \beta/2, \dot{\theta}_d) < 2\alpha < f(\theta_d + \alpha + \beta/2, \dot{\theta}_d), & \dot{\theta}_d > 0 \\ \alpha - \beta/2 - 2c\dot{\theta}_d/k < \theta_d < \alpha + \beta/2, & \forall \dot{\theta}_d \end{bmatrix}\right\} \tag{28}$$

see Figure 2, and the remaining area of right contact

$$A^+_{\text{steel}} = A^+ \backslash A^+_{\text{rubber}} \tag{29}$$

as the area of right contact where the shaft behaves as a steel shaft, (23). Symmetrically we have

$$A^-_{\text{rubber}} = \left\{(\theta_d, \dot\theta_d): \begin{cases} f(\theta_d - \alpha + \beta/2, \dot\theta_d) < -2\alpha < f(\theta_d - \alpha - \beta/2, \dot\theta_d), & \dot\theta_d < 0 \\ -\alpha - \beta/2 < \theta_d < -\alpha + \beta/2 - 2c\dot\theta_d/k, & \forall \dot\theta_d \end{cases}\right\} \tag{30}$$

$$A^-_{\text{steel}} = A^- \backslash A^-_{\text{rubber}} \tag{31}$$

The area of no contact is now given by

$$A^0_{\text{rubber}} = \{(\theta_d, \dot\theta_d)\} \backslash (A^-_{\text{rubber}} \cup A^-_{\text{steel}} \cup A^+_{\text{rubber}} \cup A^+_{\text{steel}}) \tag{32}$$

The areas A^0_{rubber}, A^-_{rubber}, A^-_{steel}, A^+_{rubber} and A^+_{steel} are depicted in Figure 2(d). In the areas $A^+_{\text{steel}} \subset A^+$ and $A^-_{\text{steel}} \subset A^-$ the shaft torque should be given by (23), i.e.

$$T^+_{\text{steel}} = k(\theta_d - \alpha) + c\dot\theta_d \tag{33}$$

$$T^-_{\text{steel}} = k(\theta_d + \alpha) + c\dot\theta_d \tag{34}$$

and in A^0_{rubber} the torque T should be zero. We have now accomplished feature 2, i.e. included the rubber thickness in the model. Now let the stationary elasticity (i.e. for $\dot\theta_s = 0$) of the shaft torque $T_{\text{rubber}}(\theta_s, \dot\theta_s)$ satisfy

$$\mathrm{d}T_{\text{rubber}}(\theta_s, 0)/\mathrm{d}\theta_s = \begin{cases} k|\theta_s|/\beta, & |\theta_s| < \beta \\ k, & |\theta_s| \geqslant \beta \end{cases} \tag{35}$$

By integrating (35) and remembering the continuity feature 1, we obtain the following models valid in A^+_{rubber} and A^-_{rubber} respectively:

$$T^+_{\text{rubber}} = \begin{cases} \left(\dfrac{k(\theta_d - \theta^*(\dot\theta_d) + \beta/2)}{2} + k(\theta^*(\dot\theta_d) - \alpha) + c\dot\theta_d\right)\dfrac{\theta_d - \theta^*(\dot\theta_d) + \beta/2}{\beta}, & \dot\theta_d > 0 \\ \left(\dfrac{k(\theta_d - \alpha + \beta/2}{2} + c\dot\theta_d\right)\dfrac{\theta_d - \alpha + \beta/2 + 2c\dot\theta_d/k}{\beta/2 + 2c\dot\theta_d/k}, & \dot\theta \leqslant 0 \end{cases} \tag{36}$$

$$T^-_{\text{rubber}} = \begin{cases} \left(\dfrac{k(-\theta_d + \theta^*(\dot\theta_d) + \beta/2)}{2} + k(-\theta^*(\dot\theta_d) - \alpha) + c\dot\theta_d\right)\dfrac{\theta_d - \theta^*(\dot\theta_d) - \beta/2}{\beta}, & \dot\theta_d > 0 \\ \left(\dfrac{k(-\theta_d - \alpha + \beta/2)}{2} + c\dot\theta_d\right)\dfrac{\theta_d + \alpha - \beta/2 + 2c\dot\theta_d/k}{\beta/2 - 2c\dot\theta_d/k}, & \dot\theta_d \leqslant 0 \end{cases} \tag{37}$$

For $\dot\theta_d \to 0$ or $c \to 0$ equations (36) and (37) reduce to

$$T^+_{\text{rubber}}(\theta_d, 0) = [k(\theta_d - \alpha + \beta/2)/2](\theta_d - \alpha + \beta/2)/\beta \tag{38}$$

$$T^-_{\text{rubber}}(\theta_d, 0) = [k(-\theta_d - \alpha + \beta/2)/2](\theta_d + \alpha - \beta/2)/\beta \tag{39}$$

which satisfy (35). The extended phase plane model for backlash with rubber is now given by

$$T_{\text{rubber}}(\theta_d, \dot{\theta}_d) = \begin{cases} T^+_{\text{steel}}, & (\theta_d, \dot{\theta}_d) \in A^+_{\text{steel}} \\ T^+_{\text{rubber}}, & (\theta_d, \dot{\theta}_d) \in A^+_{\text{rubber}} \\ 0, & (\theta_d, \dot{\theta}_d) \in A^-_{\text{rubber}} \\ T^-_{\text{rubber}}, & (\theta_d, \dot{\theta}_d) \in A^-_{\text{rubber}} \\ T^-_{\text{steel}}, & (\theta_d, \dot{\theta}_d) \in A^-_{\text{steel}} \end{cases} \tag{40}$$

Note that $T_{\text{rubber}}(\theta_d, \dot{\theta}_d)$ is continuous in θ_d and $\dot{\theta}_d$. $T_{\text{rubber}}(\theta_d, \dot{\theta}_d)$ is graphically expressed in Figure 2(d). Note also that if $\beta \to 0$, then the rubber model (40) converges to the phase plane model (23).

For the case where $c = 0$, the torque is independent of $\dot{\theta}_d$. A simplified model for $c = 0$ is then given by (33), (34), (38) and (39) as

$$T(\theta_d) = T_{\text{rubber}}(\theta_d, 0) = \begin{cases} k(\theta_d - \alpha), & \theta_d \geqslant \alpha + \beta/2 \\ [k(\theta_d - \alpha + \beta/2)/2](\theta_d - \alpha + \beta/2)/\beta, & \alpha - \beta/2 < \theta_d < \alpha + \beta/2 \\ 0, & |\theta_d| \leqslant \alpha - \beta/2 \\ [k(-\theta_d - \alpha + \beta/2)/2](\theta_d + \alpha - \beta/2)/\beta, & \alpha - \beta/2 < \theta_d < \alpha + \beta/2 \\ k(\theta_d + \alpha), & \theta_d \leqslant -\alpha - \beta/2 \end{cases} \tag{41}$$

This is a 'smoothed' dead-zone model where $\mathrm{d}T(\theta_d)/\mathrm{d}\theta_s$ is continuous.

4. SIMULATIONS AND MEASUREMENTS: BACKLASH WITH RUBBER

In order to test the model derived in Section 3, let us compare simulations and measurements of a speed-controlled two-mass system connected with a shaft with flexible coupling including a rubber part. The measurements were performed on a 60 kW laboratory set-up at ABB Industrial Systems AB, modelled and described in (42) and Figure 5.

$$\begin{aligned} J_m\ddot{\theta}_m &= T_{\text{control}} + a_{\text{dist}} T_{\text{base}} \sin(2\pi f_{\text{dist}} t) - T_{\text{rubber}}(\theta_d, \dot{\theta}_d) \\ J_l\ddot{\theta}_l &= mT_{\text{base}} + T_{\text{rubber}}(\theta_d, \dot{\theta}_d) \\ \theta_d &= \theta_m - \theta_l \end{aligned} \tag{42}$$

with the parameters

$J_m = 0{\cdot}4$ kg m s^{-2}	motor inertia
$J_l = 5{\cdot}6$ kg m s^{-2}	load inertia
$k = 5895$ N m rad^{-1}	shaft elasticity
$c = 3$ N m rad^{-1} s^{-1}	inner damping shaft
$\alpha = 0{\cdot}05$ rad	backlash gap
$\beta = 0.05$ rad	rubber thickness
$T_{\text{base}} = 380$ N m	nominal motor torque
$\omega_{\text{raf}} = 1438$ rev min^{-1} = 150.6 rad s^{-1}	speed reference
$a_{\text{dist}} = 0{\cdot}05$	disturbance amplitude factor
$f_{\text{dist}} = 6$ or $9{\cdot}5$ Hz	disturbance frequency
$m = -0{\cdot}06$	preload gain.

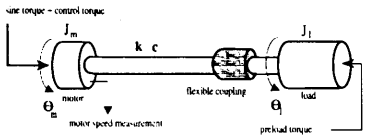

Figure 5. Laboratory set-up

The control input is the motor torque T_{control} and the measured output is the motor speed $\dot{\theta}_{\text{m}}$. The parameters in the simulation were given by mechanical data and adjusted by identification experiments with high preload torques, in which case the system is essentially linear. The backlash gap α and rubber thickness β were measured with a ruler. The original purpose of the measurements was to find an approximation of the frequency response of the system rather than to validate a simulation model. Therefore the measurements consisted of 49 swept sine experiments for different working conditions, parameterized by different constant preload gains m and different amplitudes a_{dist} of the injected sine wave. The control system was a PI controller with very flow bandwidth, which in practice will give a constant control $T_{\text{control}} = -mT_{\text{base}}$. The

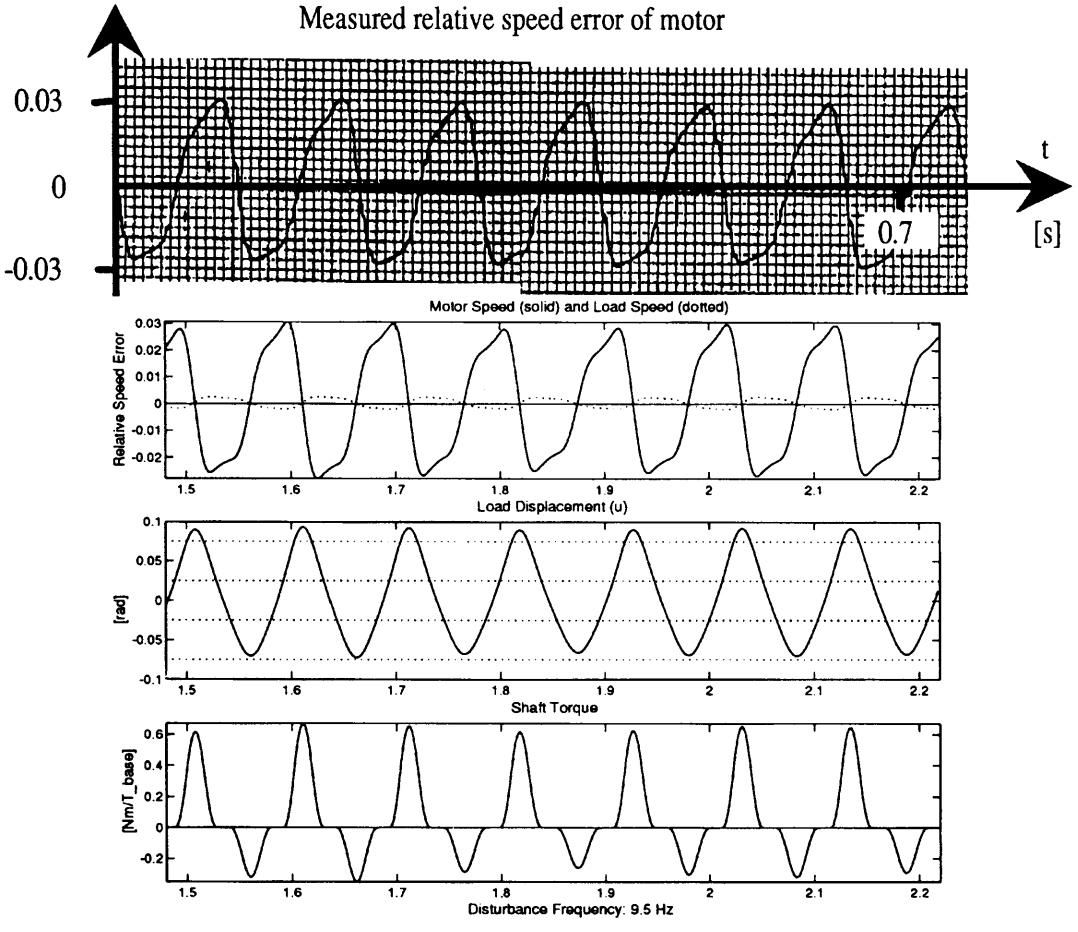

Figure 6. Measurement and simulations of system (42): 9·5 Hz. Speeds are relative to ω_{base}

motor speed θ_m and load speed θ_l will then, in steady state, vary around the speed reference ω_{ref}.

To test the simulation model, we chose a number of time domain measurements and then compared these measurements with simulations of the same system including the new model for a flexible coupling. Let us now look at the measurement and corresponding simulation in Figure 6. It can be seen that the shaft bounces between *right contact* and *left contact*.

It seems that the new model is sufficient to approximate well the behaviour of this two-mass system. Numerous other simulations and measurements for different loads and frequencies fit very well to measurements. Some of these are presented in Reference 12, including modes with persisting right contact where the measured behaviour only depends on the rubber thickness.

5. CONCLUSIONS

In order to design an efficient control system, by any method, for a mechanical system including non-smooth non-linearities such as backlash, it seems necessary to have a correct model. Hitherto the dead-zone model[1-4] has been used for designs reported in the literature, such as classical design using the describing function,[10,17,18,20-22] robust linear design using the describing function,[13] linear design with a load observer,[6] switching robust design with a load sensor[14] or adaptive control using an inverse model.[11] In this paper it is shown that the dead-zone model is wrong, even giving the wrong sign of the driving torque, for the case of an elastic shaft with internal damping. Designs based on the hysteresis model are reported in References 10 and 11. The hysteresis model, however, is not suitable when there are disturbances acting on the load side, owing to loss of causality.

A new exact model for an inertia-free elastic shaft with internal damping connected to a backlash is presented in this paper. The model includes a state for the shaft twist. A simplified stateless model is derived from the exact model, giving the shaft torque as a function of the displacement between the driving and driven members, θ_d, and its time derivative $\dot{\theta}_d$.

The model is also extended to the 'flexible coupling' case when the backlash gap is partly filled with rubber.

After some easily satisfied simplifying assumptions, the new model is compared by analysis and simulations with the exact torque solution and the dead-zone model.

It is shown that the new model gives a negligible torque error in comparison with the exact torque solution. In Reference 12 a longer version of this paper is presented. There describing function methods are used to analyse the phase plane model. In comparison with the dead-zone model, the new model exhibits a significant phase lag, which might indicate the possibility of previously unpredicted limit cycles.

For the flexible coupling case, simulations of the new model were compared with measurements of a 60 kW laboratory system. The results were strikingly similar; see Reference 12 for further examples.

The new model seems to represent the physical backlash sufficiently well for control purposes and should replace the prevalent but erroneous dead-zone model for analysis and design. In contrast with the dead-zone model, the new model cannot be replaced by an equivalent uncertain linear gain plus a bounded disturbance.[13-15] Hence the above-mentioned robust and adaptive techniques probably have to be modified. An attempt in this direction is reported in Reference 16.

We believe that the new model will serve well as the basis for development of robust and adaptive control algorithms for mechanical systems with backlash.

ACKNOWLEDGEMENTS

This work was supported by NUTEK Grant 93-01763.

REFERENCES

1. Tustin, A., 'Effects of backlash and of speed dependent friction on the stability of closed-cycle control systems', *J. IEE*, **94**, pt. 2A 143–151 (1947).
2. Liversidge, J. H., *Backlash and Resilience within Closed Loop of Automatic Control Systems*, Academic, New York, 1952.
3. Chestnut, H. and R. W. Mayer, *Servomechanisms and Regulating System Design*, Wiley, New York, 1955, pp. 257, 301–321.
4. Cosgriff, R. L., *Nonlinear Control Systems*, McGraw-Hill, Reading, MA, 1958, pp. 121–123, 193–194.
5. Brandenburg, G., 'Stability of a speed controlled elastic ,two-mass system with backlash and Coulomb friction and optimization by a load observer', *Proc. Symp. on Modelling and Simulations for Control of Lumped and Distributed Parameter Systems*, France Depot Legal, Grenoble Lille, 1986, pp. 107–113 1987.
6. Brandenburg, G., 'Stability problems of a speed controlled drive in an elastic system with backlash and corrective measures by a load observer', *Proc. Int. Conf. on Electrical Machines*, Munich, September 1986, pp. 596–527. IFAG
7. Brandenburg, G., 'State position control for elastic pointing and tracking systems with gear play and Coulomb friction—a summary of results', *Proc. Eur. Conf. on Power Electronics and Applications*, Firenze, October, 1989, pp. 596–602. Litagrafia, GEDA, Torino, Italy
8. Brandenburg, G. and U. Schäfer, 'Influence and partial compensation of backlash for a position controlled elastic two-mass system', *Proc. Eur. Conf. on Power Electronics and Applications*, Grenoble, September 1987, pp. 1041–1047.
9. Brandenburg, G. and U. Schäfer, 'Influence and adaptive compensation simultaneously acting backlash and Coulomb friction in elastic two-mass systems of robots and machine tools', *Proc. ICCON '89*, Jerusalem, 1989, IEEE, New York, 1989, pp. WA-4SCR5.
10. Gelb, A. and W. E. Vander Velde, *Multiple-Input Describing Functions and Nonlinear System Design*, McGraw-Hill, New York, 1968.
11. Tao, G. and P. Kokotovic, 'Adaptive control of systems with backlash', *Automatica*, **29**, 323–335 (1994).
12. Nordin, M., *Licenciate Thesis, trita*/mat-95-os3, Royal Institute of Technology, Stockholm, 1995.
13. Oldak, S., C. Baril and P.-O. Gutman, 'Quantative design of a class of nonlinear systems with parameter uncertainty', *Int. J. Robust Nonlinear Control*, **4**, 101–117 (1994).
14. Boneh, R. and O. Yaniv, 'Control of an elastic two-mass system with large backlash', *Master's Thesis*, Department of Electronic Systems, Tel Aviv University, 1994.
15. Peschon, J., *Disciplines and Techniques of Systems Control*, Blaisdell, New York, 1965.
16. Nordin, M. and P.-O. Gutman, 'A robust linear design of an uncertain two-mass system with backlash', *Proc. 1st IFAC Workshop in Automotive Control*, Ascona, Italy, 1995, pp. 183–88.
17. Atherton, D. P., *Nonlinear Control Engineering*, Van Nostrand Reinhold, New York, 1975.
18. Atherton, D. P., *Stability of Nonlinear Systems*, Wiley, New York, 1981.
20. Freeman, E. A., 'An approximate transient analysis of a second order position-control system when backlash is present', *Institution Monograph 254*, Institution of Electrical Engineers, London, 19057.
21. Freeman, E. A., 'Stabilization of control systems with backlash using a high-frequency on–off loop', *Institution Monograph 356*, Institution of Electrical Engineers, London, 1957.
22. Freeman, E. A., 'The effect of speed dependent friction and backlash on the stability of automatic control systems', *Trans. Am. IEE*, **7**, (1958).